Langmuir

Article

Controlling Clusters of Colloidal Platelets: Effects of Edge and Face Surface Chemistries on the Behavior of Montmorillonite Suspensions

William J. Ganley and Jeroen S. van Duijneveldt*

School of Chemistry, University of Bristol, Cantock's Close, Bristol BS8 1TS, U.K.

S *Supporting Information*

ABSTRACT: The structural and rheological consequences of adsorbing pyrophosphate anions to the edges and polyether-amines to the faces of montmorillonite platelets in aqueous suspension were investigated. Oscillatory rheology and scattering experiments showed that the two surface treatments act in different regions of the phase diagram and that this can be attributed to modifications of local particle interactions resulting in changes to the behavior and morphology of platelet clusters. The polyetheramine was found to neutralize surface charge, reducing electrostatic repulsion between platelets and therefore allowing them to come into closer proximity. This reduces the effective volume fraction of the clusters and reverses jamming in low ionic strength arrested phases. Conversely, the adsorption of pyrophosphate was found to introduce a high concentration of negative charge to the particle edge, resisting the formation of bonded percolating gels at high ionic strength. The two separate surface chemistries can be applied in parallel with no adverse effects and thus have the potential to be applied to dual functionalization of two-dimensional colloids such as platelets. This has implications for finer formulation design where targeted rheology modification could be achieved by careful selection of chemistry at one surface accompanied by an additional function at the other.

INTRODUCTION

Anisotropic colloidal particles have been the subject of many recent studies due to their unusual behavior. Such particles have the potential to form complex self-organized structures[1] and have been reported to give rise to phases such as cluster fluids, gels, and glasses,[2,3] empty liquids, and equilibrium gels.[4]

Clay minerals disperse into liquids to form suspensions of particles with a variety of shapes such as rods,[5] plates,[6] and laths.[7] These suspensions present a wealth of phase behavior ranging from fluids to delicate liquid crystalline phases and unusually low volume fraction viscoelastic glassy or gelled states. This has led to widespread use for rheology modification in pharmaceutical, agrochemical, cosmetic, and drilling fluid formulations, as fillers in paper production, and in nano-composite materials. The smectite clay montmorillonite swells and delaminates in water to give suspensions of high aspect ratio platelets (300:1) and has been the subject of extensive studies into the rheological and structural characteristics of suspensions of nonspherical particles.[2,8−16]

An isotropic to nematic transition is expected for hard particles with such a high aspect ratio;[17,18] however, due to strong electrostatic interactions, resulting from isomorphous substitutions in the clay mineral structure,[10] arrested states such as gels or glasses are observed instead. The exact interactions causing this phase behavior have been debated since these suspensions were first reported.[19−22] Simulations involving nonlinear charge screening,[23] point quadrupoles within the particles,[24] dipoles along the plane of the particles,[25] and patchy interactions around the particles[4] have all been employed to reproduce experimental findings.

The rheological phase behavior of montmorillonite was experimentally mapped out in detail by Abend and Lagaly,[11] and a re-entrant phase transition was observed from a disconnected glassy state to a fluid and then a connected network gel as ionic strength increased. This soft solid behavior at low volume fraction has been attributed to either strong electrostatic repulsion between the highly negatively charged particles (see refs 26 and 27 for a detailed discussion of this for a related clay mineral) at low ionic strength and attractive percolating gels (due to van der Waals forces or electrostatic interactions) which fill space at high ionic strength. Unusual flow behavior as a result of particle anisometry has also been explored by considering a hydrodynamic effective volume fraction due to rotation of the particles about their central axis.[28,29]

While there is no full consensus over the interactions between clay platelets, it is known that their behavior can be modified by adsorbing molecules to the particle surface. Amphiphilic polymers,[30−33] anionic polymers,[34−36] zwitter-ions,[37] anions,[38−40] and more recently amine anchored polymers[41,42] have been used to liquefy the solid states formed by these suspensions in a variety of conditions. However, very few of these studies explore the microstructure within the

suspensions, stemming from the alteration in particle–particle interactions, which dictates the macroscopic phase behavior.

It has recently been shown that montmorillonite platelets undergo microphase separation into clusters[2] as observed in systems with competing interactions such as colloid–polymer mixtures[43] and natural protein solutions.[44] Considerations of the dynamics of these clusters correlate well with the bulk rheological phase behavior. Additionally, Cui et al. observed changes in the morphology of the clusters upon the adsorption of an amine terminated polymer to the platelet faces which correlated with liquefaction of the gelled suspensions.[41] This begs the question as to whether structural modifications at the largest scale are a common feature across the plethora of surface chemistries used to modify the rheology of montmorillonite suspensions. If so, knowledge of the exact structural consequences of platelet surface chemistry would lead to a better understanding of the interactions within these systems and to more directed design of formulations containing platelet particles.

We approach this by taking two surface chemistries already reported to drastically change the behavior of aqueous montmorillonite dispersions: the face adsorbing amine-terminated polymer Jeffamine M1000 discussed above[41] and the edge adsorbing anion pyrophosphate which has been long used for this purpose.[38,39] Rheological phase diagrams of montmorillonite platelets with or without these surface chemistries are plotted and correlated with scattering measurements at a variety of length scales. It is found that these two species alter behavior in different regions of the phase diagram and that this can be correlated with large scale structures observed in small-angle light scattering.

■ EXPERIMENTAL SECTION

Materials. Wyoming montmorillonite (SWy-2) was purchased from the Clay Minerals Society source clays repository at Purdue University. The composition of SWy-2 is $(Si_{7.94}Al_{0.06})$-$(Al_{2.88}Fe_{0.5}Mg_{0.62})O_{20}(OH)_4Na_{0.68}$,[12] and it has a cation exchange capacity of 84 mequiv/100 g.[45] Jeffamine M1000 was donated by Huntsman and has the molecular structure $CH_3[OCH_2CH_2]_{19}$-$[OCH_2CH_3CH]_3NH_2$ and a molecular weight of ~1000 g mol^{-1}. Reagent grade NaCl was purchased from Fischer, and reagent grade $Na_4P_2O_7 \cdot 10H_2O$ was purchased from Sigma-Aldrich.

Sample Preparation. Montmorillonite was dispersed by adding 45 g L^{-1} powdered clay to deionized water and stirring for 24 h. The suspension was then dialyzed against aqueous NaCl (1 M) for 1 week, changing the solution every day, to remove unwanted ions such as Ca^{2+}, and then dialyzed against deionized water, changing water every day, until the conductivity of the dialysate was below 5 μS cm^{-1}. The dialyzed suspension was centrifuged at 7000 rpm (5500g) for 60 min in a Sorvall Legend-T to remove large impurities. The supernatant was kept as stock, and its weight percentage was measured by weight loss upon drying at 60 °C under vacuum for 5 h. The samples were prepared at natural pH of 8.5 though this increased somewhat upon addition of the weakly basic sodium pyrophosphate.

Samples for rheological measurements were prepared by concentrating stock suspensions by evaporation (if required) and then diluting into aqueous solutions of M1000 (added at 340 μmol per g of montmorillonite to ensure minimal free polymer[45]), $Na_4P_2O_7$, and NaCl.

Samples for scattering measurements were prepared by first diluting the stock suspension, prepared as above, to 1 wt % and allowing larger particles to settle under gravity for 24 h and keeping the supernatant as stock suspension. This prevented time-dependent variations in scattering intensity due to particle sedimentation. The weight percentage of this new stock suspension was determined as above,

and the suspension was diluted into appropriate salt and polymer solutions.

Exfoliation of platelets by this dispersion method was assessed by viewing suspensions between crossed polars. Birefringence was observed, consistent with the presence of platelike objects. This was even true at the highest ionic strength (0.1 M Na$^+$) showing strong evidence for the presence of either free platelets, or possibly very small stacks, but not large aggregates of particles, agreeing with previous birefringence and X-ray scattering measurements.[9,13,16] See the Supporting Information for images of birefringent samples.

Characterization. Structural characterization was carried out using a range of scattering techniques. Static light scattering (SLS) was carried out using a Malvern 4800 Autosizer where the intensity of light scattered from a 532 nm laser was measured at angles from 30° to 140°, corresponding to the wavevector range 6×10^{-3} to 2×10^{-2} nm^{-1}. Samples were diluted into a 10 mm cylindrical quartz cell with deionized water passed through a 0.22 μm Whatman filter.

Small-angle light scattering (SALS) was measured using home-built apparatus based on the designs of Verhaegh et al.[46] and Schätzel and Ackerson[47] using a 5 mW, $\lambda = 632.8$ nm He–Ne laser. The sample was diluted as above into a 1 mm path length rectangular glass cell, the laser beam was directed through the sample, and scattered light was projected onto a screen with a central hole for the incident beam to pass through. An image of the scattering pattern was collected using a Stringray F125B ASG camera with a CCTV lens at 646 × 482 pixels and a bit depth of 16. The transmission intensity was measured using a photodiode behind the screen. Data acquisition and reduction was performed using homemade NI LabVIEW 2011 (with IMAQdx) applications, and the apparatus was calibrated using a 100 lines/mm diffraction grating. Angles from 0.6° to 12° were probed corresponding to wavevectors from 10^{-4} to 2×10^{-3} nm^{-1}

Small-angle X-ray scattering (SAXS) was collected on the I9115 beamline at the MAXII storage ring at Max5Lab (Lund, Sweden) using a wavelength of $\lambda = 0.091$ nm and a PILATUS 1 M detector. Data were normalized to the intensity of the incident beam and corrected for detector efficiency using Bli711 software,[48] and water background was subtracted using PRIMUS software.[49]

Because of multiple scattering in SLS and SALS, only dilute samples of 0.1 and 0.25 wt %, respectively, could be used. Samples for SAXS were prepared at 1 wt % to allow comparison with other techniques.

The phase diagrams were determined by following the elastic (G') and viscous (G'') moduli of suspensions as a function of shear amplitude and frequency in oscillatory rheological measurements. Montmorillonite suspensions in M1000 and NaCl or $Na_4P_2O_7$ solutions at weight fractions ranging from 2 to 5 wt % and sodium ion concentrations (C_{Na^+}) ranging from 10^{-1} to 10^{-5} M corresponding either to the concentration of NaCl or one-quarter of that of $Na_4P_2O_7$ were examined. Measurements were carried out using a Malvern Kinexus Pro rheometer controlled by rSpace software. Samples were presheared at 30 s^{-1} for 300 s and then rested for 300 s before each measurement. An amplitude sweep was carried out from 0.01 to 10 Pa at 1 Hz (or 0.1 Hz if samples were too liquid-like) recording 11 points per decade with a minimum integration time of 10 s. The lowest stable stress in the linear viscoelastic region was selected, and a frequency sweep was measured from 10 to 0.1 Hz recording 11 points per decade with a minimum integration time of 10 s. Measurements for phase diagrams used a cone and plate geometry (40 mm diameter, 4°) to maximize frequency range.

The effects of pyrophosphate adsorption and characterization of surface chemistry combinations were determined by measuring amplitude sweeps after preshear as above and recording the plateau elastic modulus (G'_0). An unroughened parallel plate geometry (20 mm diameter, 1 mm gap) was used to minimize wall slip. See the Supporting Information for an examination of the extent of wall slip for the two geometries.

Electrophoretic mobility was measured using a Brookhaven Zeta Plus instrument and an aqueous dip cell. Suspensions were measured at Na$^+$ ion concentrations of 10^{-1} M to minimize double-layer contributions.

■ RESULTS

Adsorption of M1000 and Pyrophosphate. Large changes in the shape of the rheological phase diagrams of montmorillonite are observed upon the adsorption of M1000 to the particle faces or pyrophosphate anions to the particle edges. This is accompanied by significant changes to the organization of the particles and their electrophoretic mobility.

The measured electrophoretic mobility, shown in Table 1, shows a drop upon the adsorption of M1000 and increases

Table 1. Electrophoretic Mobility of 0.25 wt % Montmorillonite Suspensions in 10^{-1} M Na$^+$

surface functionalization	μ (10^{-8} m^2 V^{-1} s^{-1})
untreated	-1.43 ± 0.08
M1000	-1.07 ± 0.10
pyrophosphate	-2.50 ± 0.10

upon the addition of pyrophosphate. This is consistent with expectations as the amine terminus of the M1000 polymer has previously been shown to neutralize one unit of charge per molecule adsorbed,[45] and the adsorption of pyrophosphate is thought to introduce 3 units of charge per molecule adsorbed. Amine-terminated polyethers have been reported to adsorb to the negatively charged montmorillonite platelet surface by first undergoing an acid−base reaction with acidified water molecules at the particle surface (in the presence of Na$^+$ in the particle double layer acting as a Lewis acid). The resulting ammonium cation then bonds electrostatically to the particle surface.[45]

Pyrophosphate anions are commonly accepted to adsorb at the platelet edge surface,[38] and this is often explained as being due to either electrostatic attraction between the negatively charged anion and the positively charged edge surface or an ion exchange process.[39] Edge isoelectric points up to pH 7[50,51] have been reported; therefore, it can be assumed that the edge surfaces in the present systems (prepared at pH > 8) are not positively charged and adsorption is due to an ion exchange mechanism between hydroxyl ions, capping broken Al−O and Si−O bonds at the crystal terminus, and pyrophosphate anions. The pyrophosphate and hydroxyl anions in this instance are bound to formally cationic Si^{4+} and Al^{3+} atoms; therefore, this adsorption could not occur at the particle face as this surface carries a negative charge.

A previous study measured the adsorption of pyrophosphate on kaolin using atomic absorption spectroscopy and radiotracer techniques and reported adsorbed amounts in the region of a few μmol g^{-1}.[52] There has yet to be a detailed study using such techniques, or others such as infrared spectroscopy, to determine the detailed adsorption mechanism for pyrophosphate on montmorillonite. However, based on the platelet structure, the case for edge adsorption is plausible and is assumed here as it has been in many past studies on this clay.[36,38,39]

The effect of pyrophosphate adsorption on montmorillonite was probed indirectly by measuring the amount of anion required to liquefy a high ionic strength gel (see Figure 1). Assuming a direct relationship between adsorption and rheological behavior, the data in Figure 1 can be fitted to the form of a Langmuir adsorption isotherm using the empirical relationship shown in eq 1, where G_0' is the measured plateau modulus, G_{max}' is the plateau modulus in the absence of
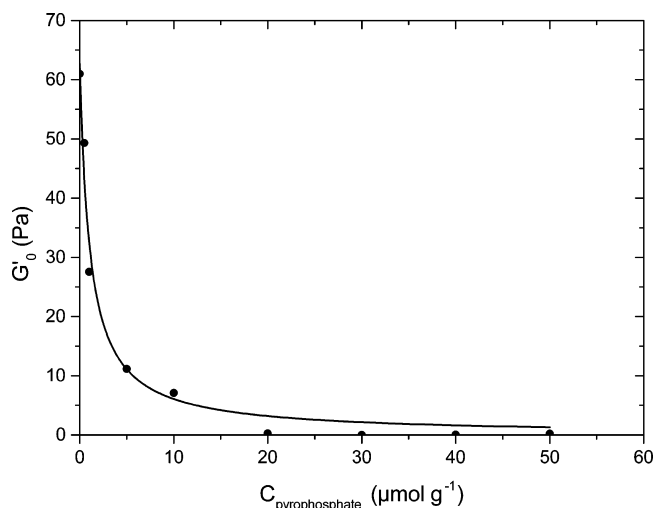

Figure 1. Plateau elastic modulus of 2 wt % montmorillonite suspensions in 10^{-1} M NaCl with increasing amounts of pyrophosphate measured at a rotational frequency of 0.1 Hz. The solid line is a fit to eq 1.

pyrophosphate, C_p is the concentration of pyrophosphate, and α is a fitting parameter.

$$G_0' = G_{max}'\left(1 - \frac{\alpha C_p}{1 + \alpha C_p}\right) \qquad (1)$$

Figure 1 shows that the concentration of pyrophosphate required to minimize G_0' is 20 μmol g^{-1}, an order of magnitude lower than the adsorption of M1000 to the particle face (M1000 adsorbs at 340 μmol g^{-1}), which could be explained by the pyrophosphate adsorbing only to the edges of the particles.

Rheological Behavior of Functionalized Montmorillonite. Adsorption of M1000 and pyrophosphate has been found to drastically alter the rheology of aqueous montmorillonite suspensions away from the classic re-entrant behavior reported by Abend and Lagaly.[11] The phase behavior is captured for untreated montmorillonite and that treated with M1000 and pyrophosphate in Figure 2. The phase definitions follow those used by Chambon and Winter to describe polymer gels: the solid region is defined as that for which $G' > G''$ in the linear viscoelastic regime across the range of frequencies measured; the fluid region that where $G' < G''$ and the transition region is defined as a system where the moduli cross over in the range of observed frequencies.[53]

The raw rheological data corresponding to these diagrams can be found in the Supporting Information, and of note is that even at the highest C_{Na^+} the magnitude of the viscoelastic moduli is not reduced for the untreated and M1000-treated samples. This indicates that the particles are present as individual platelets (or small stacks) exhibiting large effective volume fractions due to their high aspect ratio. If they were present as aggregates, the free volume available to the platelets would be much greater and the suspensions would exhibit a much reduced elastic response. The pyrophosphate samples do in fact show a reduced modulus at high ionic strength; however, it is likely that this is due to the electrostatic repulsion that the anions introduce between the platelets opposing attractive network formation and not due to the showing extensive aggregation, and this agrees with the observation of birefringence in these samples.
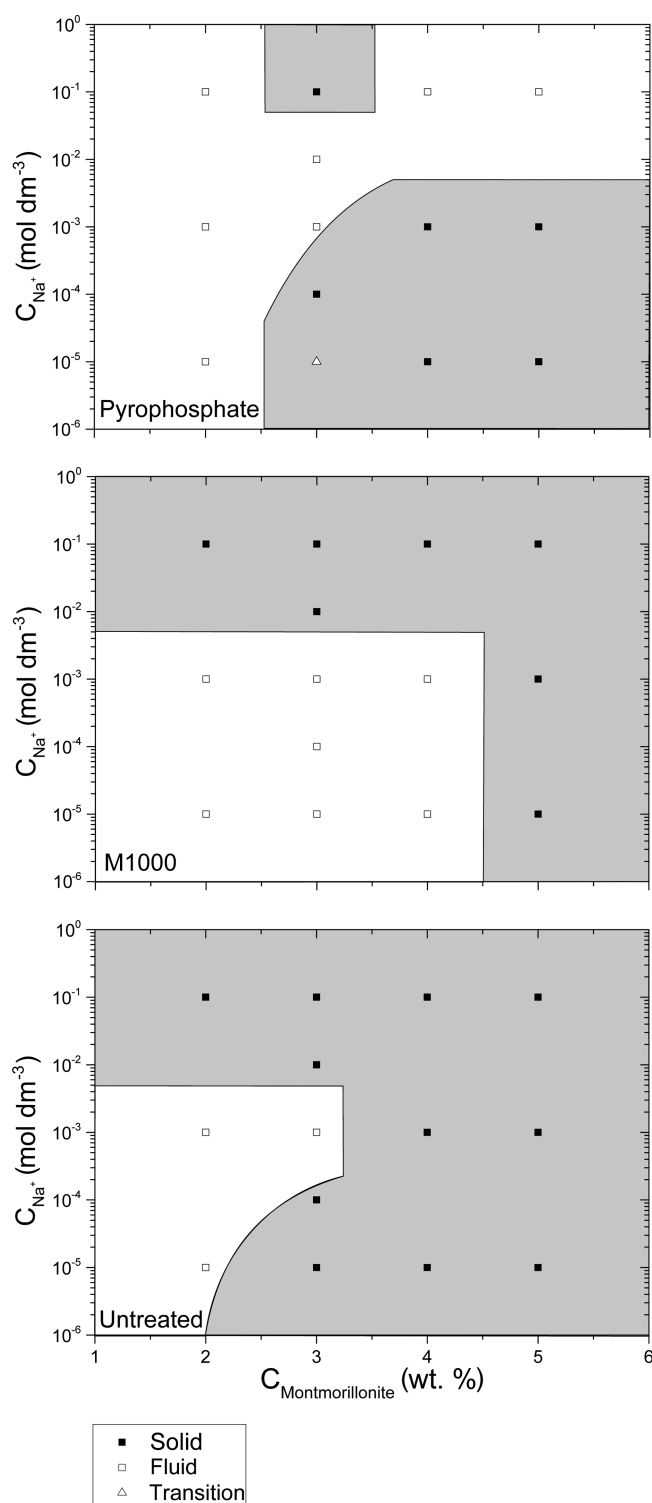
Figure 2. Rheological phase diagram for untreated montmorillonite suspensions in NaCl solution (lower), treated with 340 μmol g^{-1} M1000 in NaCl solution (middle) and pyrophosphate treated where Na$_4$P$_2$O$_7$ has been added in place of NaCl (upper). Filled points represent the solid phase ($G' > G''$), and open points represent fluid regions ($G' < G''$). Coloring is a guide to the eye.

Figure 2 shows that the adsorption of M1000 induces a solid to fluid transition only at low ionic strength. The adsorption of pyrophosphate results in a solid to fluid transition at high ionic strength, though the lack of effect at low ionic strength may be

due to the lack of phosphate in the system as the added Na$^+$ corresponds to one-quarter of the P$_2$O$_7^{4-}$ concentration.

These phase diagrams show the overall behavior of this system in a clear manner; however, there are subtleties which this classification does not capture. Measurements where G' and G'' are in the same order of magnitude may be subject to variations in relative magnitude due to small differences in sample composition or environment which could cause a sample to be classified differently. That said, even with this simple binary classification system the phase diagrams still show striking differences in behavior between the surface chemistries, highlighting the significance of their corresponding modifications.

To study the possibility of a system with both edge and face surface functionalization, the plateau elastic moduli (G_0') at 1 Hz of 5 wt % montmorillonite suspensions with none, one, or both of the surface chemistries were measured. The measurements were carried out at high C_{Na^+}, where pyrophosphate is effective, and low C_{Na^+}, where M1000 is effective. The results are shown in Table 2. Note that the low C_{Na^+} systems were

Table 2. Plateau Elastic Moduli of 5 wt % Montmorillonite Suspensions with None, Either, or Both of the Surface Chemistries at High and Low C_{Na^+}

$C_{Na^+} = 10^{-1}$ M		$C_{Na^+} = 4 \times 10^{-3}$ M	
surface chemistry	G_0' (Pa)	surface chemistry	G_0' (Pa)
none	2430	none	195
pyrophosphate	1.83	pyrophosphate	319
M1000	3770	M1000	60.3
both	2.08	both	56.8

prepared at 4×10^{-3} M corresponding to the plateau region of Figure 1 so that an effective amount of anion was present in the pyrophosphate-containing samples.

Table 2 shows that the edge and face surface chemistries are compatible but show no synergy with the overall modulus being dictated by the most effective surface chemistry for a given C_{Na^+}. The modulus of low C_{Na^+} pyrophosphate-treated solid phases is reduced from 319 to 56.8 Pa when M1000 is also present. The reverse is true at high C_{Na^+} where the plateau modulus falls by 3 orders of magnitude when pyrophosphate is present even in the presence of M1000, which alone results in a higher modulus.

Table 2 also shows an increase in elastic modulus at low C_{Na^+} when only pyrophosphate is adsorbed and at high ionic strength when only M1000 is adsorbed. This suggests that these surface chemistries act not only to liquefy suspensions as shown in Figure 2 but also to rigidify the systems at the opposite end of the C_{Na^+} scale.

Small-Angle X-ray and Static Light Scattering. It was recently shown that the structure observed in scattering measurements of dilute montmorillonite suspensions correlates with flow behavior in more concentrated systems.[2,41] The following sections show characterization of the effects of surface chemistry on the structure of these suspensions at a variety of length scales in order to couple these effects to the rheological behavior detailed above.

Figure 3 shows SAXS of dilute montmorillonite suspensions with and without adsorbed M1000 or pyrophosphate at a weight fraction of 1% and low ionic strength. At the measured wavevectors a $I(Q) \propto Q^{-2}$ power law is observed for all surface chemistries. This is consistent with the presence of a two-
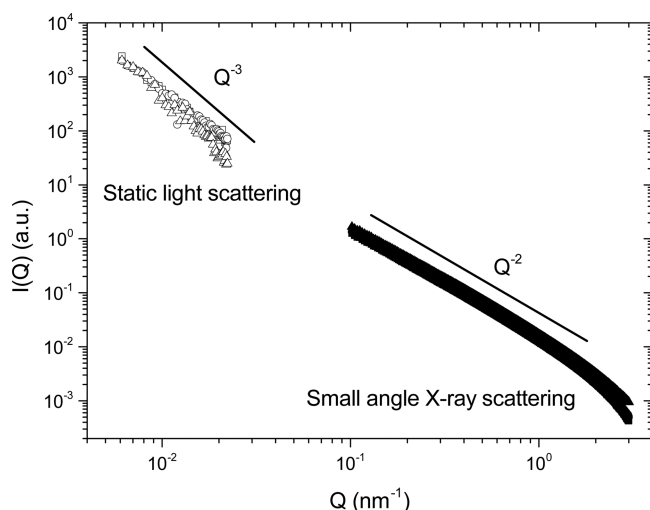
Figure 3. SLS (open symbols) of 0.1 wt % montmorillonite and SAXS (closed symbols) of 1 wt % montmorillonite in 10^{-4} M NaCl (squares), 10^{-4} M NaCl with 340 μmol g^{-1} M1000 (circles), or 10^{-4} M Na$_4$P$_2$O$_7$ (squares).

dimensional disclike object, and the lack of any high Q correlation peaks shows that our preparation methods can result in fully exfoliated platelets. Detailed studies have found evidence for particle stacks at higher particle weight fractions and ionic strengths,[13,14,16] meaning that the most basic units of the large structures we observe may exist, in more concentrated samples, as either single platelets or small stacks. However, based on the consistently high values of G' in these regions of the phase diagram, it is likely that any particle stacking be minimal if it occurs at all.

At a lower range of wavevectors, observed using SLS, a turnover to a Guinier region would be expected and has previously been observed for suspensions of platelets.[54] However, Figure 3 shows an upturn to power law with exponent between −2.5 and −3. This shows that over the observed length scales of 300−1000 nm (roughly 1−3 particle diameters) the platelets are not completely free but are loosely associated into assemblies which are either not fully smooth or not fully solid and leads to the observed scaling.[55] Such cluster assemblies agree well with previous observations of untreated platelets showing particle correlations in SAXS at distances of the particle diameter and below.[14] At even lower Q the larger scale of these clusters is observed, and it is these structures that have the greatest bearing on the rheological properties of the system.

Small-Angle Light Scattering. At these very large length scales significant structural differences as a result of functionalizing the different surfaces of the platelets are observed. Figure 4 shows the SALS of montmorillonite with and without the two surface treatments at $C_{Na^+} = 10^{-4}$ M. Untreated montmorillonite shows a power law close to $I(Q) \propto Q^{-1}$, in line with previous observations,[41] suggestive of a large elongated assembly.

The addition of M1000 causes the system to become homogeneous at the largest length scales. This results in a low Q Guinier region and a decrease in the transmitted light intensity (see Supporting Information for % transmissions), suggesting smaller, denser scattering objects. The scattering from the M1000-treated samples can be fitted to the Fisher−Burford form factor (see eq 2) describing the scattering of
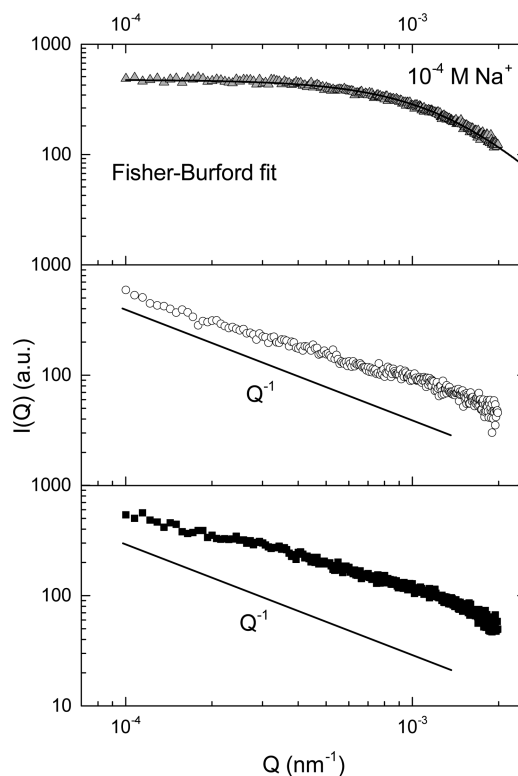

Figure 4. SALS of 0.25 wt % montmorillonite suspensions with 10^{-4} M added Na$^+$. Untreated montmorillonite represented by black squares, with 340 μmol g^{-1} M1000 (gray triangles) or in Na$_4$P$_2$O$_7$ (open circles). M1000 data are fitted to the Fisher−Burford model, and $I(Q) \propto Q^{-1}$ power laws are shown on other data sets.

cluster assemblies with fractal dimension d_f and radius of gyration R_g.

$$I(Q) = I(0)\left[1 + \frac{2(QR_g)^2}{d_f}\right]^{-d_f/2} \tag{2}$$

This has previously been used to model the scattering of clusters formed by montmorillonite suspensions at pH 4 and aggregating silica.[2,56] Fits of the Fisher−Burford equation to M1000-treated montmorillonite are shown in Figures 4 and 5 using $d_f = 2.7$ (from SLS), yielding radii of gyration around 500 nm (see Supporting Information for full details).

At high ionic strength, scattering from the M1000-treated particles is no longer captured by the Fisher−Burford model (the attempted fit can be seen as the solid line in the upper plot in Figure 5) as the particles begin to form aggregates with large scale inhomogeneities. The untreated montmorillonite can actually be captured by the Fisher−Burford form factor at high ionic strength, suggesting changes in structure away from the elongated assemblies observed at lower ionic strength. The results of fits to SALS across the full range of ionic strengths can be found in the Supporting Information.

Such a drastic difference is not observed for the pyrophosphate-treated particles. At low ionic strength this system follows the same $I(Q) \propto Q^{-1}$ power law as the untreated system, suggestive of elongated assemblies. Structural changes resulting from the adsorption of pyrophosphate anions become more apparent at the highest ionic strength measured; here Figure 5 shows that the cluster structure for the untreated platelets changes to one which fits the Fisher−Burford form,
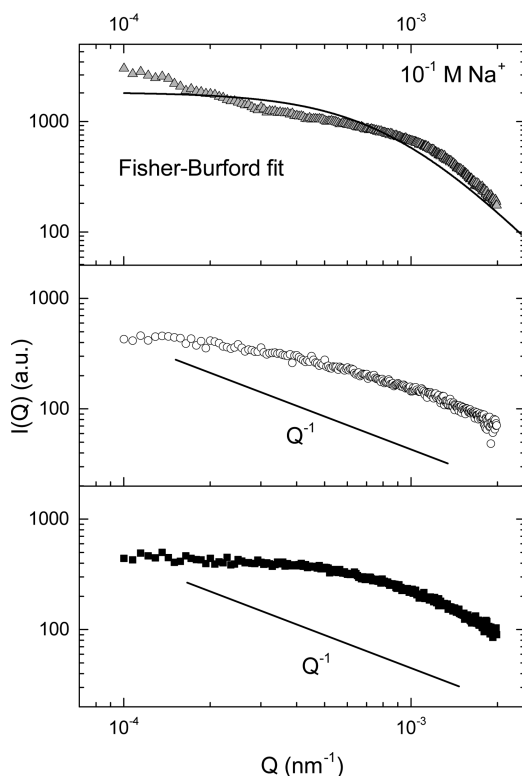
Figure 5. SALS of 0.25 wt % montmorillonite suspensions with 10^{-1} M added Na^+. Untreated montmorillonite represented by black squares, with 340 μmol g^{-1} M1000 (gray triangles) or in $Na_4P_2O_7$ (open circles). M1000 data are fitted to the Fisher–Burford model, and $I(Q) \propto Q^{-1}$ power laws are shown on other data sets.

but the pyrophosphate scattering shows a partial transition between this and the $I(Q) \propto Q^{-1}$ power law. Such a difference is even more pronounced at $C_{Na^+} = 10^{-2}$ M (see Supporting Information). This shows that the reorganization of the untreated system at high ionic strength occurs to a lesser extent when the particle edges are decorated with the highly valent anions.

■ DISCUSSION

Small-angle light scattering measurements (Figures 4 and 5) show evidence for clusterlike assemblies of various morphologies formed by montmorillonite platelets (or small stacks of platelets) in aqueous suspension. This is a result of competing attractive and repulsive interactions inherent in the particles (as discussed in the Introduction) and mirrors other natural[2,44] and model[57,58] colloidal systems.

Clusters occur where short-range attractions, favoring nearest-neighbor contacts, bring particles together but are balanced by the presence of a longer range electrostatic repulsion, preventing complete phase separation. The growing assemblies therefore have a certain electrostatic self-energy preventing growth beyond the point where the attractive and repulsive forces balance. This microphase-separated state can be described as a suspension of loose clusters, which prevail as the largest objects in the system, and hence define its flow properties. Tipping the balance of these forces can have large effects on the morphology of the colloidal clusters and therefore the flow properties of the system as a whole, and this is what is observed when the interactions between platelets

are modified by adsorbing different species to the particle surface.

Shalkevich et al. previously studied montmorillonite suspensions at pH 4 where edges are likely to be positively charged and hence form electrostatically bonded networks at lower weight fractions than fluid to solid transitions observed in this study.[2] They suggested the existence of a cluster fluid (observed in light scattering) at low particle weight fraction that undergoes dynamic arrest as weight fraction increases, either by the formation of a cluster glass at low ionic strength where electrostatic repulsions dominate or a system spanning percolating network, which eventually phase separates, at very high ionic strength.

Figures 4 and 5 confirm the existence of clusters in the dilute suspensions studied here, the morphology and response to ionic strength of which are altered by changing the surface chemistry of the particles. This is consistent with the changes to rheological phase diagrams (see Figure 2) and suggests a link between particle interactions, suspension structure, and bulk rheology.

The clusters observed by light scattering in the untreated montmorillonite system have the characteristics of elongated assemblies (as observed previously[41]). Upon increasing weight fraction at low ionic strength the clusters become more numerous and jam due to strong electrostatic repulsion between them. This results in arrest of the system and is observed in the phase diagram at high weight fraction and low ionic strength. At high ionic strength charge is screened, and the clusters are allowed to come into closer proximity where attractive interactions between particles are strongest and the clusters fuse, causing the system to tend to a solid network phase. At the natural pH of these systems (~8) the particle edges are unlikely to be charged; therefore, the nature of this attractive interaction lies in more complex multipolar moments inherent in the charge sandwich structure of the mineral previously discussed for similar clay particles.[24,25]

The adsorption of the amine-terminated amphiphilic polymer M1000 to the face surface of these platelets results in neutralization of one unit of surface charge per polymer chain adsorbed. This is observed as a reduction in the electrophoretic mobility of the particles (see Table 1). Such a change in surface charge tips the balance of attractive and repulsive interactions by reducing electrostatic repulsion between individual particles and hence the self-energy of the clusters. Smaller denser clusters are favored at the same weight fraction which show a decrease in transmitted intensity (see Supporting Information) in light scattering measurements compared to the more diffuse elongated clusters and can be captured by applying the Fisher–Burford form factor (see solid lines in Figures 4 and 5). These denser clusters have a lower effective volume fraction than an equivalent suspension of untreated montmorillonite and hence have more free volume to diffuse into causing the system to undergo a transition from the solid to the fluid state at low ionic strength. At high ionic strength the clusters undergo a similar fusion to that of the untreated particles. This is observed as very low Q features in the high ionic strength regime seen in Figure 5. These are qualitatively different than that of the untreated montmorillonite, which has no very low Q features at this ionic strength but still results in a rigid connected solid system observed in rheological measurements (see Figure 2). The differences in scattering could be due to clusters of different morphologies fusing to form different system spanning, connected networks.
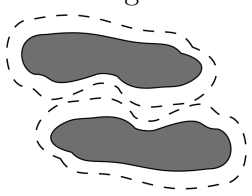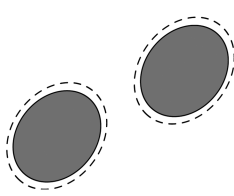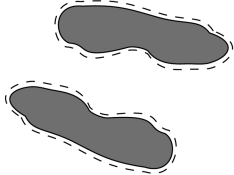
Salt Concentration	Structure in Solid State	Structure in Fluid State
Low C_{Na^+}	Arrested elongated clusters	Fluid of dense clusters
	Untreated and pyrophosphate treated	M1000 treated
High C_{Na^+}	Percolating gel	Fluid of elongated clusters
	Untreated and M1000 treated	Pyrophosphate treated

Figure 6. Large-scale structures relating to high and low salt regions of rheological phase diagrams at medium weight fraction (~3 wt %): the gray region represents location of platelets or small stacks of platelets (though their true arrangement is unknown), and dotted lines represent electrostatic repulsion between platelets (this is not to scale).

The resulting systems therefore show different inhomogeneities in their structure which may result in the different plateau elastic moduli shown in Table 2. Figure 6 shows the differences in behavior between untreated and M1000 treated systems schematically.

Parallels can be drawn between this system and those that have been reported to show cluster sizes varying with particle volume fraction.[59,60] Here the dominating effect is surface charge neutralization by adsorption of the amine-terminated polymer. This is analogous to previous observations of changes in cluster morphology due to counterion condensation upon an increasing particle volume fraction.[59] Both of these effects reduce the repulsive electrostatic component of particle interactions, increasing the relative magnitude of the attractive interaction and therefore increasing the number of particles associated with a stable cluster.

The addition of pyrophosphate to the particle edges has a different effect entirely. Figure 2 shows that the adsorption of these highly valent anions to the particle edges causes a solid to fluid transition in the high ionic strength region of the phase diagrams. This is due to the introduction of three units of charge per pyrophosphate anion adsorbed which is observed as an increase in electrophoretic mobility of the particles (see Table 1). At high ionic strength stronger electrostatic repulsion prevents the particles from coming into close enough contact for the large scale bonded network to form. Hence, the clusters retain some mobility until their effective volume fraction exceeds unity. Deviations from the $I(Q) \propto Q^{-1}$ behavior at high ionic strength are lesser when the platelet edges are decorated with anions. Table 2 shows that adsorption of pyrophosphate anions at low ionic strength actually enhances rigidity compared to the untreated system, suggesting that the presence of this anion impacts upon rheological behavior, despite a lesser structural difference observed in Figure 4, which may be due to an increased repulsive force between the jammed clusters.

The two surface chemistries studied act in different regions of the phase diagram by either the introduction or the neutralization of surface charge. This allows for particles with functionalization on both the edge and face surfaces to be prepared with no impairment to the liquefying effect of either treatment. For example, high ionic strength suspensions of M1000-treated montmorillonite can be prepared in the fluid state if pyrophosphate anions are also adsorbed to the particle edges opposing gelation, and conversely low ionic strength fluid suspensions of pyrophosphate-treated montmorillonite can be prepared by the addition of M1000 to the particle face to neutralize surface charge and loosen the cluster glass state. This is seen upon comparison of the plateau elastic moduli for single and mixed surface treatment systems shown in Table 2.

This may be advantageous in situations where the properties of one type of surface functionalization are desired but such a functionalization would place the system in the wrong physical state for the application. For example, polymers related to M1000 such as poly(ethylene oxide) and diamino polyether-amines have been reported for use as shale inhibitors in water-based drilling fluids; however, these systems may undergo fluid to solid transitions at high ionic strength. Further functionalization of the edge surface with pyrophosphate would allow for rheological control while retaining the function of the shale inhibiting polymer.

■ CONCLUSIONS

It has been shown that behavior and structure at the largest length scales in aqueous suspensions of montmorillonite can be manipulated by adsorbing different molecules to the face and edge surfaces. Figure 2 shows that adsorption to different surfaces of the platelets causes liquefaction in opposite regions of the phase diagrams, and SALS measurements, shown in Figures 4 and 5, show that this is a result of changes in the behavior of clusters of platelets (or small stacks of platelets) brought on by manipulation of the interactions between particles.

The untreated platelets are found to form elongated cluster assemblies which can either jam by electrostatic repulsion or fuse to form system spanning networks at high weight fractions. Adsorption of the polyetheramine Jeffamine M1000 to the

platelet face surface neutralizes surface charge, resulting in liquefaction in the low ionic strength electrostatically jammed regime. Adsorption of highly valent anions to the particle edge surface was found to prevent gelation at high ionic strength by introducing additional electrostatic resistance to the formation of attractive bonded networks.

The surface chemistries also act in the presence of each other with no impairment to rheological modification. This methodology could therefore be used for dual functionalization of the platelets and applied to systems where one type of surface chemistry is used for a desired function and the other to optimize this function by tuning physical properties. Examples include shale inhibiting drilling fluids containing fully exfoliated platelets with a high salt tolerance and Pickering emulsion stabilizers with both controlled wettability and the potential for further chemistry at the interface.

Understanding the behavior of this system from particle interactions to large-scale structures to bulk rheological properties has revealed important detail regarding the surface chemistry of anisotropic colloidal particles. Building upon previous work on the clustering behavior clay platelets,[2,41] this work has expanded the understanding by considering exactly how the largest scale structures can be manipulated by changing particle interactions and how this, in turn, affects the rheological properties of the system. The precise intracluster organization of the platelets, leading to the scaling observed in SLS, is still unknown. This could be investigated using SAXS on a wide range of samples (similar to studies conducted on untreated platelet colloids[13,14,16]) and would provide a more detailed understanding for the hierarchical structures formed by anisometric colloidal particles with competing interactions. This would make interesting further work.

Consideration of the separate surfaces has the potential for expansion beyond the rheological modification presented here toward a functional system with high level of fine-tuning of both chemical and physical properties.

■ ASSOCIATED CONTENT

Ⓢ Supporting Information
Observations of suspensions between crossed polars, full rheological frequency sweeps used to produce phase diagrams shown in Figure 2, additional small-angle light scattering data for an extended range of ionic strengths with fitting data and corresponding transmitted light measurements, and analysis of wall slip extent for geometries used in rheological measurements. This material is available free of charge via the Internet at http://pubs.acs.org.

■ AUTHOR INFORMATION

Corresponding Author
*E-mail J.S.Van-Duijneveldt@bristol.ac.uk (J.S.v.D.).

Notes
The authors declare no competing financial interest.

■ ACKNOWLEDGMENTS

■ REFERENCES

(1) Glotzer, S. C.; Solomon, M. J. Anisotropy of building blocks and their assembly into complex structures. *Nat. Mater.* **2007**, *6*, 557−562.

(2) Shalkevich, A.; Stradner, A.; Bhat, S. K.; Muller, F.; Schurtenberger, P. Cluster, glass, and gel formation and viscoelastic phase separation in aqueous clay suspensions. *Langmuir* **2007**, *23*, 3570−3580.

(3) Atmuri, A.; Bhatia, S. Polymer-mediated clustering of charged anisotropic colloids. *Langmuir* **2013**, *29*, 3179−3187.

(4) Ruzicka, B.; Zaccarelli, E.; Zulian, L.; Angelini, R.; Sztucki, M.; Moussaïd, A.; Narayanan, T.; Sciortino, F. Observation of empty liquids and equilibrium gels in a colloidal clay. *Nat. Mater.* **2011**, *10*, 56−60.

(5) Zhang, Z. X.; van Duijneveldt, J. S. Isotropic-nematic phase transition of nonaqueous suspensions of natural clay rods. *J. Chem. Phys.* **2006**, *124*, 154910.

(6) Paineau, E.; Antonova, K.; Baravian, C.; Bihannic, I.; Davidson, P.; Dozov, I.; Impéror-Clerc, M.; Levitz, P.; Madsen, A.; Meneau, F.; Michot, L. J. Liquid-crystalline nematic phase in aqueous suspensions of a disk-shaped natural beidellite clay. *J. Phys. Chem. B* **2009**, *113*, 15858−15869.

(7) Michot, L. J.; Baravian, C.; Bihannic, I.; Maddi, S.; Moyne, C.; Duval, J. F. L.; Levitz, P.; Davidson, P. Sol-gel and isotropic/nematic transitions in aqueous suspensions of natural nontronite clay. influence of particle anisotropy. 2. Gel structure and mechanical properties. *Langmuir* **2008**, *25*, 127−139.

(8) Ramsay, J. D. F.; Lindner, P. Small-angle neutron scattering investigations of the structure of thixotropic dispersions of smectite clay colloids. *J. Chem. Soc., Faraday Trans.* **1993**, *89*, 4207−4214.

(9) Gabriel, J.-C. P.; Sanchez, C.; Davidson, P. Observation of nematic liquid-crystal textures in aqueous gels of smectite Clays. *J. Phys. Chem.* **1996**, *100*, 11139−11143.

(10) Luckham, P. F.; Rossi, S. The colloidal and rheological properties of bentonite suspensions. *Adv. Colloid Interface Sci.* **1999**, *82*, 43−92.

(11) Abend, S.; Lagaly, G. Sol-gel transitions of sodium montmorillonite dispersions. *Appl. Clay Sci.* **2000**, *16*, 201−227.

(12) Michot, L. J.; Bihannic, I.; Porsch, K.; Maddi, S.; Baravian, C.; Mougel, J.; Levitz, P. Phase diagrams of Wyoming Na-montmorillonite clay. Influence of particle anisotropy. *Langmuir* **2004**, *20*, 10829−10837.

(13) Segad, M.; Jönsson, B.; Åkesson, T.; Cabane, B. Ca/Na montmorillonite: Structure, forces and swelling properties. *Langmuir* **2010**, *26*, 5782−5790.

(14) Paineau, E.; Bihannic, I.; Baravian, C.; Philippe, A.-M.; Davidson, P.; Levitz, P.; Funari, S. S.; Rochas, C.; Michot, L. J. Aqueous suspensions of natural swelling clay minerals. 1. Structure and electrostatic interactions. *Langmuir* **2011**, *27*, 5562−5573.

(15) Paineau, E.; Michot, L. J.; Bihannic, I.; Baravian, C. Aqueous suspensions of natural swelling clay minerals. 2. Rheological characterization. *Langmuir* **2011**, *27*, 7806−7819.

(16) Michot, L. J.; Bihannic, I.; Thomas, F.; Lartiges, B. S.; Waldvogel, Y.; Caillet, C.; Thieme, J.; Funari, S. S.; Levitz, P. Coagulation of Na-montmorillonite by inorganic cations at neutral pH. A combined transmission X-ray microscopy, small angle and wide angle X-ray scattering study. *Langmuir* **2013**, *29*, 3500−3510.

(17) Onsager, L. The Effects of shape on the interaction of colloidal particles. *Ann. N. Y. Acad. Sci.* **1949**, *51*, 627−659.

(18) Veerman, J. A. C.; Frenkel, D. Phase behavior of disklike hard-core mesogens. *Phys. Rev. A* **1992**, *45*, 5632−5648.

(19) Van Olphen, H. Rheological phenomena of clay sols in connection with the charge distribution on the micelles. *Discuss. Faraday Soc.* **1951**, *11*, 82−84.

(20) Norrish, K. The swelling of montmorillonite. *Discuss. Faraday Soc.* **1954**, *18*, 120−134.

(21) Callaghan, I. C.; Ottewill, R. H. Interparticle forces in montmorillonite gels. *Faraday Discuss. Chem. Soc.* **1974**, *57*, 110−118.

(22) Rand, B.; Pekenc, E.; Goodwin, J. W.; Smith, R. W. Investigation into the existence of edge-face coagulated structures in Na-montmorillonite suspensions. *J. Chem. Soc., Faraday Trans. 1* **1980**, *76*, 225−235.

(23) Agra, R.; Trizac, E.; Bocquet, L. The interplay between screening properties and colloid anisotropy: towards a reliable pair potential for disc-like charged particles. *Eur. Phys. J. E: Soft Matter Biol. Phys.* **2004**, *15*, 345−57.

(24) Dijkstra, M.; Hansen, J. P.; Madden, P. A. Gelation of a clay colloid suspension. *Phys. Rev. Lett.* **1995**, *75*, 2236−2239.

(25) Fartaria, R.; Javid, N.; Pethrick, R. A.; Liggat, J. J.; Sefcik, J.; Sweatman, M. B. Structure of laponite-styrene precursor dispersions for production of advanced polymer-clay nanocomposites. *Soft Matter* **2011**, *7*, 9157−9166.

(26) Kroon, M.; Wegdam, G. H.; Sprik, R. Dynamic light scattering studies on the sol-gel transition of a suspension of anisotropic colloidal particles. *Phys. Rev. E* **1996**, *54*, 6541−6550.

(27) Ruzicka, B.; Zulian, L.; Zaccarelli, E.; Angelini, R.; Sztucki, M.; Moussaïd, A.; Ruocco, G. Competing Interactions in Arrested States of Colloidal Clays. *Phys. Rev. Lett.* **2010**, *104*, 85701.

(28) Baravian, C.; Vantelon, D.; Thomas, F. Rheological determination of interaction potential energy for aqueous clay suspensions. *Langmuir* **2003**, *19*, 8109−8114.

(29) Philippe, A. M.; Baravian, C.; Bezuglyy, V.; Angilella, J. R.; Meneau, F.; Bihannic, I.; Michot, L. J. Rheological study of two-dimensional very anisometric colloidal particle suspensions: From shear-induced orientation to viscous dissipation. *Langmuir* **2013**, *29*, 5315−5324.

(30) Parfitt, R.; Greenland, D. The adsorption of poly (ethylene glycols) on clay minerals. *Clay Miner.* **1970**, *8*, 305−315.

(31) Burchill, S.; Hall, P. L.; Harrison, R.; Hayes, M. H. B.; Langford, J. I.; Livingston, W. R.; Smedley, R. J.; Ross, D. K.; Tuck, J. J. Smectite-polymer interactions in aqueous systems. *Clay Miner.* **1983**, *18*, 373−397.

(32) Nelson, A.; Cosgrove, T. Small-angle neutron scattering study of adsorbed pluronic tri-block copolymers on laponite. *Langmuir* **2005**, *21*, 9176−9182.

(33) Rossi, S.; Luckham, P. F.; Tadros, T. F. Influence of non-ionic polymers on the rheological behaviour of Na+-montmorillonite clay suspensions. Part II. Homopolymer ethyleneoxide and polypropylene oxide-polyethylene oxide ABA copolymers. *Colloids Surf., A* **2003**, *215*, 1−10.

(34) Labanda, J.; Llorens, J. Influence of sodium polyacrylate on the rheology of aqueous Laponite dispersions. *J. Colloid Interface Sci.* **2005**, *289*, 86−93.

(35) Akimkhan, A. M. Adsorption of polyacrylic acid and polyacrylamide on montmorillonite. *Russ. J. Phys. Chem. A* **2013**, *87*, 1875−1880.

(36) Bergaya, F.; Lagaly, G. *Handbook of Clay Science*; Elsevier Science: Amsterdam, 2013.

(37) Schmidt, C. U.; Lagaly, G. Surface modification of bentonites: I. Betaine montmorillonites and their rheological and colloidal properties. *Clay Miner.* **1999**, *34*, 447−447.

(38) Van Olphen, H. *An Introduction to Clay Colloid Chemistry: For Clay Technologists, Geologists, and Soil Scientists*; Krieger Publishing Company: Malabar, FL, 1991.

(39) Penner, D.; Lagaly, G. Influence of anions on the rheological properties of clay mineral dispersions. *Appl. Clay Sci.* **2001**, *19*, 131−142.

(40) Mongondry, P.; Nicolai, T.; Tassin, J.-F. Influence of pyrophosphate or polyethylene oxide on the aggregation and gelation of aqueous laponite dispersions. *J. Colloid Interface Sci.* **2004**, *275*, 191−196.

(41) Cui, Y.; Pizzey, C. L.; van Duijneveldt, J. S. Modifying the structure and flow behaviour of aqueous montmorillonite suspensions with surfactant. *Philos. Trans. R. Soc., A* **2013**, *371* (1988), 20120262.

(42) Zhao, C.; Tong, K.; Tan, J.; Liu, Q.; Wu, T.; Sun, D. Colloidal properties of montmorillonite suspensions modified with polyether-amine. *Colloids Surf., A* **2014**, *457*, 8−15.

(43) Sedgwick, H.; Egelhaaf, S. U.; Poon, W. C. K. Clusters and gels in systems of sticky particles. *J. Phys.: Condens. Matter* **2004**, *16*, S4913.

(44) Stradner, A.; Sedgwick, H.; Cardinaux, F.; Poon, W. C. K.; Egelhaaf, S. U.; Schurtenberger, P. Equilibrium cluster formation in concentrated protein solutions and colloids. *Nature* **2004**, *432*, 492−495.

(45) Cui, Y.; van Duijneveldt, J. S. Adsorption of polyetheramines on montmorillonite at high pH. *Langmuir* **2010**, *26*, 17210−17217.

(46) Verhaegh, N. A. M.; van Duijneveldt, J. S.; Dhont, J. K. G.; Lekkerkerker, H. N. W. Fluid-fluid phase separation in colloid-polymer mixtures studied with small angle light scattering and light microscopy. *Phys. A (Amsterdam, Neth.)* **1996**, *230*, 409−436.

(47) Schätzel, K.; Ackerson, B. J. Density fluctuations during crystallization of colloids. *Phys. Rev. E* **1993**, *48*, 3766−3777.

(48) Knaapila, M.; Svensson, C.; Barauskas, J.; Zackrisson, M.; Nielsen, S. S.; Toft, K. N.; Vestergaard, B.; Arleth, L.; Olsson, U.; Pedersen, J. S.; Cerenius, Y. A new small-angle X-ray scattering set-up on the crystallography beamline I711 at MAX-lab. *J. Synchrotron Radiat.* **2009**, *16*, 498−504.

(49) Konarev, P. V.; Volkov, V. V.; Sokolova, A. V.; Koch, M. H. J.; Svergun, D. I. PRIMUS: a Windows PC-based system for small-angle scattering data analysis. *J. Appl. Crystallogr.* **2003**, *36*, 1277−1282.

(50) Durán, J. D. G.; Ramos-Tejada, M. M.; Arroyo, F. J.; González-Caballero, F. Rheological and electrokinetic properties of sodium montmorillonite suspensions: I. Rheological properties and inter-particle energy of interaction. *J. Colloid Interface Sci.* **2000**, *229*, 107−117.

(51) Pecini, E. M.; Avena, M. J. Measuring the isoelectric point of the edges of clay mineral particles: The case of montmorillonite. *Langmuir* **2013**, *29*, 14926−14934.

(52) Bidwell, J.; Jepson, W.; Toms, G. The interaction of kaolinite with polyphosphate and polyacrylate in aqueous solutions - some preliminary results. *Clay Miner.* **1970**, *8*, 445−459.

(53) Chambon, F.; Winter, H. H. Networks stopping of crosslinking reaction in a PDMS polymer at the gel point. *Polym. Bull.* **1985**, *503*, 499−503.

(54) Zhang, Z.; van Duijneveldt, J. S. Effect of suspended clay particles on isotropic-nematic phase transition of liquid crystal. *Soft Matter* **2007**, *3*, 596.

(55) Schmidt, P. Small-angle scattering studies of disordered, porous and fractal systems. *J. Appl. Crystallogr.* **1991**, 414−435.

(56) Dietler, G.; Aubert, C.; Cannell, D. S.; Wiltzius, P. Gelation of colloidal silica. *Phys. Rev. Lett.* **1986**, *57*, 3117−3120.

(57) Sedgwick, H.; Kroy, K.; Salonen, A.; Robertson, M. B.; Egelhaaf, S. U.; Poon, W. C. K. Non-equilibrium behavior of sticky colloidal particles: beads, clusters and gels. *Eur. Phys. J. E: Soft Matter Biol. Phys.* **2005**, *16*, 77−80.

(58) Campbell, A. I.; Anderson, V. J.; van Duijneveldt, J. S.; Bartlett, P. Dynamical arrest in attractive colloids: The effect of long-range repulsion. *Phys. Rev. Lett.* **2005**, *94*, 208301.

(59) Groenewold, J.; Kegel, W. K. Anomalously large equilibrium clusters of colloids. *J. Phys. Chem. B* **2001**, *105*, 11702−11709.

(60) Buitenhuis, J.; Dhont, J. K. G.; Lekkerkerker, H. N. W. Static and dynamic light scattering by concentrated colloidal suspensions of polydisperse sterically stabilized boehmite rods. *Macromolecules* **1994**, *27*, 7267−7277.